

# Economical Treatments of Relativistic Effects and Electron Correlation in $\text{WH}_6$

ROLAND H. HERTWIG,<sup>1</sup> WOLFRAM KOCH<sup>1\*</sup>, BRIAN F. YATES<sup>2\*</sup>

<sup>1</sup>*Institut für Organische Chemie, Technische Universität Berlin, Straße des 17. Juni 135, D-10623 Berlin, Germany*

<sup>2</sup>*School of Chemistry, University of Tasmania, GPO Box 252C, Hobart TAS 7001, Australia*

Received 24 April 1998; accepted 15 June 1998

**ABSTRACT:** The equilibrium geometries and relative stabilities of several structural isomers of tungsten hexahydride,  $\text{WH}_6$ , have been obtained at different levels of quantum chemical calculations. The performance of various strategies to (i) include electron correlation, *viz.* density functional theory based approaches, Møller/Plesset perturbation and coupled cluster theory, and to (ii) account for scalar relativistic effects, *viz.* various relativistic effective core potentials, first order perturbation theory, a quasi-relativistic treatment employing a Pauli Hamiltonian, and use of the Douglas/Kroll operator, are compared to the best theoretical data available. It is shown that relativistic and electron correlation effects are most important for the high-symmetry species, that these effects give rise to opposite trends in relative energies, and that overall the relativistic effects dominate. The most efficient way to incorporate relativistic effects appears to be via the use of relativistic effective core potentials, while the correlation energies are best taken account of using a conventional method such as CCSD(T). © 1998 John Wiley & Sons, Inc. *J Comput Chem* 19: 1604–1611, 1998

**Keywords:** electron correlation; relativistic effects; tungsten hexahydride

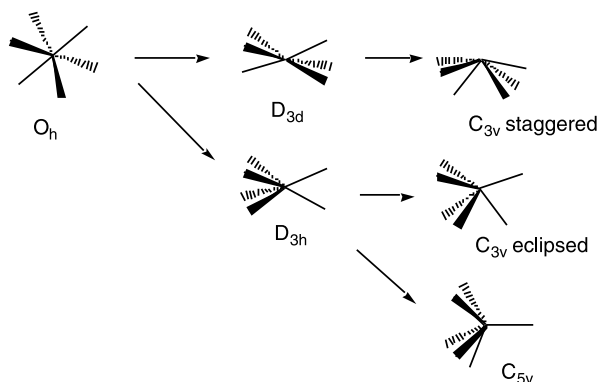
## Introduction

**T**ungsten hexahydride is one of the prototype molecules of  $d^0 \text{ML}_6$  complexes and its peculiar geometrical features have attracted consider-

able attention in the past. In particular, it was noted very early that  $\text{WH}_6$  as well as other  $d^0 \text{ML}_6$  complexes do not adhere to the valence-shell electron-pair repulsion (VSEPR) [1] rules which predict an octahedral equilibrium geometry for these species. Rather, distortions of the molecular framework occur leading to structures of lower symmetry, as indicated in Scheme 1 [2, 3]. Computational investigations of systems such as this are complicated by two well known facts. First, electron correlation has a significant impact on transi-

\* Authors for correspondence.

This article includes Supplementary Material available from authors upon request or via the Internet at <ftp.wiley.com/public/journals/jcc/suppmat/19/1604> or <http://journals.wiley.com/jcc/>



**SCHEME 1.** Distortions of the  $\text{WH}_6$  molecule.

tion metal containing compounds and a prerequisite for methods applicable to these systems is an adequate treatment of correlation (which, as a side effect, necessitates the use of large and flexible basis sets). In addition, for molecules containing heavy transition metals relativistic effects are of great importance and need to be considered as well. The geometrical and energetical aspects of the  $\text{WH}_6$  molecule have recently been investigated by several groups. Shen, Schaefer and Partridge (SSP) determined the equilibrium structures of various isomers at the Hartree-Fock level using all-electron basis sets of different quality [2]. Subsequent energy calculations utilized second order Møller/Plesset perturbation theory (MP2), the modified coupled pair approximation (MCPF) and the coupled cluster approach with single and double excitations (CCSD). Scalar relativistic effects (*i.e.*, the mass/velocity and Darwin terms) were included through first-order perturbation theory in combination with the MCPF wave functions. In a note added in proof SSP briefly mention a second set of calculations in which relativistic effective core potentials (RECP) due to Hay and Wadt were used in combination with the MCPF, CCSD and CCSD(T) methods. Both strategies lead to comparable results: Among the isomers studied, the lowest energy was obtained for a  $\text{C}_{3v}$  symmetric species with an eclipsed arrangement of the hydrogens and a  $\text{C}_{5v}$  isomer, which are essentially energetically degenerate. The  $\text{WH}_6$  molecule is also among the systems studied by Kang, Tang and Albright (KTA) in their systematic investigation on the structures of  $\text{d}^0 \text{ML}_6$  and  $\text{ML}_5$  complexes [3]. Also these authors employ the Hay and Wadt RECPs to account for the relativistic effects. The geometries are obtained at the MP2 level while the

best relative energies were computed using the quadratic configuration interaction method with singles and double excitations and a perturbative estimate of the triple substitutions (QCISD(T)). Very akin to the results of SSP, the eclipsed  $\text{C}_{3v}$  and the  $\text{C}_{5v}$  isomers are the two most stable isomers of tungsten hexahydride with the former being only  $4 \text{ kJ mol}^{-1}$  more stable than the latter. Calculations employing density functional theory using the local density approximation, the gradient corrected BLYP functional as well as the HF/DFT hybrid functional B3LYP were recently reported by Tanpipat and Baker (TB) [4]. An RECP due to Ross and coworkers with an  $[4s3p3d]$  valence basis set for tungsten was used for covering the relativistic effects. The results are again in very good agreement with those reported earlier. Based on these three sets of results, the aims of the present work are twofold: First, an accurate, reliable and yet economic strategy to include scalar relativistic and electron correlation effects is sought. To this end, different approaches to account for the spin free relativistic effects are employed, ranging from the simple use of an RECP, first order perturbation theory to a quasi-relativistic treatment employing a Pauli Hamiltonian, and finally use of the spin free Douglas/Kroll operator. Likewise, density functional theory based methods, Møller/Plesset perturbation and coupled cluster theory, are utilized to tackle the correlation problem. While we will only concentrate on  $\text{WH}_6$ , the conclusions emerging from this part of our study are most probably transferable to other, related systems. Second, we will present the most accurate structural and energetical details on the various isomers of the  $\text{WH}_6$  molecule available so far, utilizing highly correlated, relativistically corrected wave functions already for the geometry optimization.

## Computational Details

A variety of one-particle descriptions was used in this study. The major part of the calculations employed relativistic effective core potentials for describing the 60 electrons of the  $[\text{Kr}] 4d^{10}4f^{14}$  tungsten core. The RECPs were mainly taken from the work of the Stuttgart group of Stoll, Preuß and coworkers (SP) [5]. For a few comparisons at lower levels of theory we also used the RECP by Hay and Wadt (LANL2) [6] or the pseudopotential of Stevens, Krauss, Basch and Jasien

(SKBJ) [7]. The remaining fourteen 5s, 5p, 5d and 6s electrons of the transition metal were included explicitly through valence basis sets of different size, the largest consisting of a 6s5p4d3f contraction. The hydrogen basis sets associated with the RECP also range from simple double- $\zeta$  quality up to a flexible 5s2p1d contraction. The actual basis set sizes and the nomenclature used in the following are given in Table I.

Calculations with the ADF density functional program [8] treated either the [Xe] 4f<sup>14</sup> or [Kr] 4d<sup>10</sup> inner shell electrons of tungsten in the frozen core approximation while the valence electrons were expanded as linear combinations of Slater-type basis functions. Triple- $\zeta$  basis sets (ADF standard basis set IV) were used throughout. Finally, an all-electron basis set for tungsten was generated by augmenting the 24s17p15d10f primitive set of Huzinaga and Klobukowski [9] by adding three p-one d- and two f-type diffuse/polarization functions with exponents as suggested by SSP [2]. The primitive set was contracted to an 18s17p12d5f set. This tungsten one-particle basis, which is of similar quality as the largest basis set (Basis H) used by SSP, was combined with the standard 6-311G(2d,2p) basis for hydrogen (i.e., (5s2p)  $\rightarrow$  [3s2p]) [10] resulting in a total of 218 contractions for WH<sub>6</sub>.

The RECPs were utilized in geometry optimizations using the Turbomole [11], Gaussian 94 [12], MolPro96 [13] and Mulliken [4] programs at the restricted HF, MP2, and CCSD(T) levels of conventional, wave function based methodology. In addition, we used Turbomole, Gaussian 94 and Mul-

iken for utilizing approximate density functional theory employing the gradient corrected BP86 [15,16] and BLYP [17,18] functionals and the HF/DFT hybrid functional B3LYP [19]. Mulliken is particularly suited for these applications, since it is the only program known to us which provides analytical gradients if RECPs in combination with valence basis sets including f-functions are employed. Using the ADF program the STO triple- $\zeta$  basis set was used together with the BP functional. In these latter calculations the scalar relativistic effects were evaluated using the quasi-relativistic method due to Ziegler, Baerends *et al.* [20]. In this approach, a first-order Hamiltonian, obtained from the N-electron Dirac-Coulomb operator by a sequence of Foully-Wouthuysen transformations, is diagonalized in the space of the solutions to the non-relativistic, zero-order Hamiltonian. These quasirelativistic calculations employ atomic relativistic core densities, generated from the auxiliary program DIRAC [8]. Finally, the MOLCAS software [21] together with the all-electron basis set was used in combination with the MCPF approach [22] to account for electron correlation. The relativistic effects due to the mass/velocity and one-electron Darwin contact terms were explicitly treated through first order perturbation theory [23] and the spin-free Douglas/Kroll Operator [24,25,26]. At these levels of theory no geometry optimizations was performed. Rather, all energetic data are obtained by employing the equilibrium structures as identified at the CCSD(T) level combined with the RECP and the largest valence basis set (see below).

**TABLE I.**  
**Basis Sets Used in the Present Work.**

Basis set	Tungsten	Hydrogen	Full specification	No. of bf for WH <sub>6</sub>
1	Standard basis <sup>a</sup>	6-31G(d,p)	LANL2[3s3p2d]:[2s1p]	52
2	Standard basis <sup>b</sup>	6-31G(d,p)	SKBJ[4s4p3d]:[2s1p]	61
3	Standard basis <sup>c</sup>	6-31G(d,p)	ecp-60-mwb[6s5p3d]:[2s1p]	66
4	Add one f function <sup>d</sup>	6-31G(d,p)	ecp-60-mwb[6s5p3d1f]:[2s1p]	73
5	Uncontract one d function (3111) and add two f functions <sup>d</sup>	6-311G(2d,2p)	ecp-60-mwb[6s5p4d2f]:[3s2p]	109
6	Add three f functions <sup>d</sup>	Uncontract s functions and add d function	ecp-60-mwb[6s5p4d3f]:[5s2p1d]	158
7	See text	6-311G(2d,2p)	[18s17p12d5f]:[3s2p]	218

<sup>a</sup>From ref. 6. <sup>b</sup>From ref 7. <sup>c</sup>From ref 5. <sup>d</sup>The f-function exponents were optimized at UMP2 with each basis set of the s<sup>1</sup>d<sup>5</sup> state of the tungsten atom: 1f  $\alpha$  = 0.755; 2f  $\alpha$  = 0.642, and 0.411; 3f  $\alpha$  = 2.463, 0.821, and 0.274.

## Results and Discussion

Before we enter an in-depth discussion of the various aspects of the present work, we should point out that the general, qualitative trends found at all levels of approximation used in the following are in perfect harmony with the results reported earlier by SSP [2], KTA [3], and TB [4]. The most stable  $\text{WH}_6$  isomers are the eclipsed  $\text{C}_{3v}$  and the  $\text{C}_{5v}$  forms, which are almost energetically degenerate, followed by the second, staggered  $\text{C}_{3v}$  arrangement, some 30–50  $\text{kJ mol}^{-1}$  higher in energy. The  $\text{D}_{3h}$  trigonal prismatic structure comes next, at about 130–140  $\text{kJ mol}^{-1}$ . Finally, the octahedral  $\text{WH}_6$  isomer is extremely disfavored energetically and is more than 500  $\text{kJ mol}^{-1}$  less stable than the global minimum. Of these, only the two  $\text{C}_{3v}$  structures and the  $\text{C}_{5v}$  isomer are confirmed by vibrational frequency calculations to be true minima on the  $\text{WH}_6$  potential energy surface. Apart from our all-electron calculations, we performed complete geometry optimisations at all of the levels of theory discussed in this paper, including CCSD(T). Relativistic effects on the geometries are very small. Electron correlation also has little effect, except to lead to a slight increase in the distortion of the  $\text{C}_{3v}$  eclipsed species. Complete tables of geometries, total energies and frequencies are available from the authors [27].

Let us consider first the dependence of the results from the choice of the RECP and the attached valence basis set. The data obtained at the RHF

level are collected in Table II while Table III contains the results when electron correlation is included in different ways.

First, it is obvious that the choice of the RECP, whether the LANL2, which was also used in the previous investigations, or the SP implementation is employed, may have significant effects on the quality of the results if the valence basis set is not flexible enough. At the uncorrelated RHF level of approximation, the LANL2 pseudopotential shows differences as large as 152  $\text{kJ mol}^{-1}$  for the relative stability of the  $\text{O}_h$  isomer depending on the valence set attached to the RECP. Less dramatic, but still significant variations are observed for the other isomers, most notably the staggered  $\text{C}_{3v}$  species. In contrast, the SP pseudopotential seems to be much more robust with respect to the size of the valence basis. The maximum deviations occur again for the  $\text{O}_h$  isomer but amount to only 40  $\text{kJ mol}^{-1}$ . Once the tungsten valence basis set includes  $f$ -functions, both RECPs converge to essentially the same results. Also included in Table II are results obtained using the SKBJ RECP, along with those of Baker and coworkers [4] using the Ermler and Christiansen RECP [28]. A comparison of the results for the four different RECPs using very similar valence basis sets (entries 2, 5, 6 and 7 in Table II for the LANL2, SKBJ, EC60 and SP relativistic effective core potentials, respectively) demonstrates the overall similarity of these effective core potentials.

At the five correlated levels shown in Table III (BP86, BLYP, B3LYP, MP2, CCSD(T)) only the results obtained from the SP pseudopotential with

**TABLE II.** Relative Energies ( $\text{kJ mol}^{-1}$ ) of  $\text{WH}_6$  Species Calculated at RHF Level with Different Basis Sets.<sup>a</sup>

RECP and basis set	$\text{O}_h$	$\text{D}_{3h}$	$\text{C}_{3v}$ staggered	$\text{C}_{5v}$	$\text{C}_{3v}$ eclipsed
LANL2[3s3p2d]:[2s] <sup>b</sup>	527	105	46	8	0
LANL2[3s3p2d]:[2s1p]	546.8	109.3	48.5	5.5	0.0
LANL2[3s3p2d1f]:[4s2p] <sup>c</sup>	395.0	—	72.0	2.5	0.0
LANL2[4s4p3d2f]:[4s2p1d] <sup>c</sup>	412.1	—	71.1	2.5	0.0
SKBJ[4s4p3d]:[2s1p]	480.7	100.2	50.1	7.9	0.0
EC60[4s3p3d]:[2s1p] <sup>d</sup>	455.2	94.6	54.4	5.9	0.0
ecp-60-mwb[6s5p3d]:[2s1p]	441.8	87.5	56.8	4.7	0.0
ecp-60-mwb[6s5p3d1f]:[2s1p]	427.3	82.9	63.1	3.1	0.0
ecp-60-mwb[6s5p4d2f]:[3s2p]	409.8	78.7	71.9	1.0	0.0
ecp-60-mwb[6s5p4d3f]:[5s2p1d]	402.4	77.5	71.7	0.9	0.0

<sup>a</sup> Geometries were fully optimized with each basis set. <sup>b</sup> These results are from ref. 3. <sup>c</sup> These results are from ref. 2. <sup>d</sup> These results are from ref. 4.

**TABLE III.**  
**Relative Energies (kJ mol<sup>-1</sup>) of WH<sub>6</sub> Species Calculated with Various Levels of Electron Correlation.<sup>a</sup>**

Level of theory		O <sub>h</sub>	D <sub>3h</sub>	C <sub>3v</sub> staggered	C <sub>5v</sub>	C <sub>3v</sub> eclipsed
BP86	Basis 4	659.4	153.4	35.5	0.8	0.0
	Basis 5	650.2	155.2	39.9	0.1	0.0
	Basis 6	645.4	154.6	39.9	0.0	0.0
BLYP	Basis 4	622.7	134.8	47.1	-1.7	0.0
	Basis 5	611.7	135.6	50.9	-2.5	0.0
	Basis 6	606.9	134.8	50.8	-2.6	0.0
B3LYP	Basis 4	597.1	131.7	47.0	-0.6	0.0
	Basis 5	584.7	131.9	51.8	-1.7	0.0
	Basis 6	579.3	131.1	51.7	-1.7	0.0
MP2	Basis 4	614.9	147.6	26.0	2.9	0.0
	Basis 5	599.4	167.6	26.6	4.2	0.0
	Basis 6	605.4	175.2	22.8	5.0	0.0
CCSD(T)	Basis 4	579.3	124.6	37.9	0.9	0.0
	Basis 5	550.0	137.1	43.9	0.1	0.0
	Basis 6	554.7	143.9	40.4	0.7	0.0
CCSD(T) <sup>b</sup>		542.7	—	45.2	-2.5	0.0

<sup>a</sup>The basis set numbers refer to those in Table I. Geometries were fully optimized at each level of theory.  
<sup>b</sup>These results (from ref. 2) were obtained with LANL2[4s4p3d2f]:[4s2p1d] and are CCSD(T) single-point calculations on RHF-optimized geometries.

the three largest valence sets (BS4 – BS6) are included, together with the CCSD(T)/LANL2/4s4p3d2f/4s2p1d single point data on RHF geometries reported by SSP [2]. The changes in the computed relative energetics are slightly more pronounced than at the RHF level, but seem to be converged to within a few kJ mol<sup>-1</sup>. The largest effects are seen for the less stable O<sub>h</sub> and D<sub>3h</sub> isomers. For example, going from BS4 to BS6, the relative stability of the O<sub>h</sub> isomer increases by some 10–25 kJ mol<sup>-1</sup>. This change by 25 kJ mol<sup>-1</sup> is observed with the CCSD(T) method, where the energy gap between the O<sub>h</sub> and the eclipsed C<sub>3v</sub> forms drops from 579.3 to 554.7 kJ mol<sup>-1</sup>. The CCSD(T)/LANL2 results by SSP are close to our best data, however, the relative stability of the O<sub>h</sub> isomer is higher still, amounting to 542.7 kJ mol<sup>-1</sup> with respect to the eclipsed C<sub>3v</sub> species. In general, augmenting the valence basis set on tungsten induces a lowering of the relative energy of the two high energy species (O<sub>h</sub> and D<sub>3h</sub>) while increasing the relative energy of the staggered C<sub>3v</sub> species at the RHF and density functional levels of theory. Using MP2 or CCSD(T), however, the larger valence basis sets lead to an increase of the relative energy of the D<sub>3h</sub> isomer.

How does the choice of the correlation treatment affect the quality of the results? From an analysis of the data contained in Table III from this

point of view, it is obvious that correlation effects have a significant influence on the relative stabilities of the various WH<sub>6</sub> isomers, particularly the high energy ones. If we concentrate on the results obtained with our largest RECP/basis set combination, i.e. SP/BS6, and take the CCSD(T) values as reference, maximum deviations of up to 53 and 51 kJ mol<sup>-1</sup> occur using the BLYP density functional and the MP2 approach, respectively. In spite of the slightly larger maximum deviation, on the average the BLYP data are considerably closer to CCSD(T) than the MP2 ones. The best results compared to CCSD(T) are obtained with the B3LYP HF/DFT hybrid functional. These differ by at most 25 kJ mol<sup>-1</sup> from our reference values, underlining once again the promising performance of this technique for including correlation even in electronically delicate situations such as transition metal compounds. Somewhat disappointing is the rather poor performance of the MP2 model, which is not only computationally more demanding than the DFT based approaches but is usually expected to provide reasonable results for closed shell transition metal compounds. As alluded to already above, the CCSD(T) results presented by SSP [2] with the LANL2 pseudopotential and a large—albeit significantly smaller compared to our SP/BS6 combination—valence set are in good agreement with our data, indicating that if combined with

flexible valence sets these two pseudopotentials offer descriptions of comparable quality.

Up to this point spin-free relativistic effects were covered through the use of relativistic effective core potentials. In this section we will consider various other strategies for estimating these effects. To this end, we performed all-electron calculations using a sufficiently flexible basis set combined with the MCPF model to incorporate dynamic electron correlation. The mass-velocity and Darwin terms were computed either via first order perturbation theory or through the Douglas-Kroll operator. The former approach has been extensively used in the past but it is questionable whether such first-order methods are still applicable for elements from the sixth row [25]. The latter scheme, which has been developed recently mainly by Heß and coworkers seems to provide a much more robust way to include the kinematical relativistic effects and has been successfully applied to elements as heavy as ekagold ( $Z = 111$ ) [29,30]. In addition, a completely different approach was also tested, *i.e.* calculations using the non-local BP density functional in which relativistic effects were accounted for through a quasi-relativistic scheme as described in the Computational Details. The results are summarized in Table IV.

We should note first that if no RECP but rather an all-electron basis set is used in combination

with the Douglas-Kroll scheme to incorporate the relativistic effects, the RHF results are consistent with the best RECP ones (Table II), with deviations that do not exceed  $8 \text{ kJ mol}^{-1}$ .

Next, the comparison between the non-relativistic all-electron results and the results obtained with the same one- and many-particle description but where the spin-free relativistic effects are included clearly indicate that relativity not only has an important impact on the relative energies, but that it is also highly non-additive! At the non-relativistic MCPF level, the staggered  $C_{3v}$  species is almost isoenergetic with the  $C_{5v}$  structure and only some  $9 \text{ kJ mol}^{-1}$  above the global minimum, the eclipsed  $C_{3v}$  isomer. If the scalar relativistic effects are accounted for, the energy gap widens significantly and reaches  $43\text{--}45 \text{ kJ mol}^{-1}$ , similar to the results obtained at our most accurate CCSD(T)/RECP levels. At the same time, the relative stability of the  $O_h$  isomer is increased by the relativistic effects. At the RHF level, this increase amounts to  $223.5 \text{ kJ mol}^{-1}$ , if the Douglas-Kroll approach is employed. However, at the MCPF level, this effect drops down significantly, the relativistic stabilization of the  $O_h$  species is now only  $125 \text{ kJ mol}^{-1}$ . Interestingly, the first-order approach yields an energy difference between the  $O_h$  and eclipsed  $C_{3v}$  species which is more than  $100 \text{ kJ mol}^{-1}$  smaller than that obtained

**TABLE IV.**  
**Relative Energies ( $\text{kJ mol}^{-1}$ ) of  $\text{WH}_6$  Species Calculated with All-Electron Basis Sets, and with a Quasirelativistic Scheme.<sup>a</sup>**

Level of Theory	$O_h$	$D_{3h}$	$C_{3v}$ staggered	$C_{5v}$	$C_{3v}$ eclipsed
RHF/Basis 7	617.5	161.3	33.4	5.3	0.0
D-K RHF/Basis 7	394.0	72.0	57.8	−1.7	0.0
MCPF/Basis 7	676.8	212.7	8.8	6.7	0.0
MCPF + R/Basis 7	444.2	126.8	43.2	−0.7	0.0
D-K MCPF/Basis 7	551.8	144.9	44.5	5.3	0.0
MCPF + R <sup>b</sup>	574.9	122.6	43.5	−1.7	0.0
BP/[Xe]4f <sup>14</sup> [3s1p3d]:[3s1p]	989.6	249.4	8.4	7.5	0.0
BP/[Kr]4d <sup>10</sup> [5s3p3d3f]:[3s1p]	881.0	228.9	7.2	8.1	0.0
BP + R/[Xe]4f <sup>14</sup> [3s1p3d]:[3s1p]	823.1	199.3	30.8	0.8	0.0
BP + R/[Kr]4d <sup>10</sup> [5s3p3d3f]:[3s1p]	609.1	133.6	48.7	−3.0	0.0

<sup>a</sup> The all-electron calculations (see Table I for description of Basis 7) were performed with the MOLCAS program and are single-point calculations on CCSD(T)/Basis 6-optimized geometries. “D-K” indicates that the Douglas–Kroll operator was used, whereas “MCPF + R” indicates that first-order perturbation theory was used to include relativistic effects. The BP and BP + R calculations were performed with the ADF program and involved complete geometry optimizations at each level of theory. “BP + R” indicates that relativistic core densities and a quasirelativistic scheme were used to include relativistic effects.

<sup>b</sup> These results (from ref. 2) were obtained with “Basis F” [19s17p11d4f]:[4s2p], and are MCPF + R single-point calculations on RHF-optimized structures.

with the Douglas-Kroll formalism, the latter being also in perfect agreement with our best CCSD(T)/RECP data (551.8 and 554.7 kJ mol<sup>-1</sup>, respectively). Similarly, the stability of the  $D_{3h}$  species as obtained with an estimation of the mass/velocity and Darwin terms by first-order perturbation theory is some 20 kJ mol<sup>-1</sup> greater than the predictions given by the CCSD(T)/RECP and MCPF/all-electron-Douglas-Kroll schemes. The MCPF results by SSP [2], where the relativistic effects were covered through first-order perturbation theory are similar to ours, with the exception of the relative stability of the  $O_h$  structure. SSP predict this isomer to be 574.9 kJ mol<sup>-1</sup> above the  $C_{3v}$  minimum, while we arrive at 444.2 kJ mol<sup>-1</sup>. The agreement between the CCSD(T)/RECP results with those obtained from the MCPF scheme combined with a large all-electron basis set and the Douglas-Kroll scheme is indeed remarkable and the difference never exceeds 5 kJ mol<sup>-1</sup>. This is a very encouraging result and enhances the level of confidence that can be attributed to our final computational predictions. After all, the two sets of data have been generated with two completely different approaches, which differ in the way the electron correlation is covered (CCSD(T) and MCPF), the one-particle description (RECP and a large all-electron basis set) and even how the spin-free relativistic effects are being accounted for (RECP and Douglas-Kroll scheme). At the same time, the above analysis supports the statement that first-order methods are probably already beyond their limits for elements from the sixth row [25] and may lead to questionable results.

The results obtained from the BP functional and the quasi-relativistic scheme as implemented in the ADF program are quite reasonable so long as a small frozen core is used (last entry in Table IV). At this level of theory, the relative stability of the  $O_h$  species, 609.1 kJ mol<sup>-1</sup>, is about 55 kJ mol<sup>-1</sup> higher than our most accurate MCPF and CCSD(T) data. The deviations for the other species are much less. At the on-relativistic level, the energy gap between the  $O_h$  and the eclipsed  $C_{3v}$  species is a rather large 881 kJ mol<sup>-1</sup>, more than 200 kJ mol<sup>-1</sup> larger than at the non-relativistic MCPF level of approximation. If the scalar relativistic effects are included the changes in the relative stabilities follow the same trend as found for the other methods, i.e., the  $O_h$  and  $D_{3h}$  forms are stabilized while the staggered  $C_{3v}$  isomer is destabilized and the stability of the  $C_{5v}$  species is only slightly changed with respect to the eclipsed  $C_{3v}$  minimum. On the whole, there is good agreement

between the results obtained with the BP functional and the quasi-relativistic scheme and those obtained using a BP/RECP approach (see the BP86 results in Table III and similar results reported by Kaupp [31]). The relative energy of the  $O_h$  isomer with the quasi-relativistic scheme is somewhat better (taking the CCSD(T)/BS6 result as our benchmark), but the deviations for the other species are similar in both approaches. The quasi-relativistic results are almost identical to those obtained with the BLYP/BS6 combination. Finally we note that very bad results are obtained if a large frozen core is used (Table IV). The non-relativistic energy gap between the  $O_h$  and the eclipsed  $C_{3v}$  species of 990 kJ mol<sup>-1</sup> drops to 823 kJ mol<sup>-1</sup> when scalar relativistic effects are included, but this is still nearly 300 kJ mol<sup>-1</sup> higher than our most accurate values. Clearly small frozen cores are important for these species.

From the above analysis of the role of relativistic effects, electron correlation and basis set dependence we can summarize the main consequences for the order of stabilities for the  $WH_6$  species (always with respect to the eclipsed  $C_{3v}$  species) as follows. Electron correlation raises the relative energy of the  $O_h$  and the  $D_{3h}$  species while it lowers the energy of the staggered  $C_{3v}$  isomer. These qualitative trends apply to the non-relativistic as well as to the relativistic case, even though there are differences in quantitative terms. The inclusion of scalar relativistic effects induces changes which frequently point in the opposite direction: The  $O_h$  and  $D_{3h}$  structures are lowered, while the staggered  $C_{3v}$  form is raised in energy. Again, these trends apply to the RHF as well as to the correlated levels of theory, with small differences in the actual quantitative amount of the variations. On combining the opposing trends of electron correlation and relativity, it is found that, overall, relativistic effects dominate for the  $O_h$  and  $D_{3h}$  species leading to an overall increase of the relative stability, while the effects of correlation and relativity approximately cancel for the staggered  $C_{3v}$  isomer inducing only little change between the non-relativistic RHF and the relativistic correlated data. For example, at the non-relativistic all-electron RHF level, the  $O_h$  isomer is 617.5 kJ mol<sup>-1</sup> less stable than the eclipsed  $C_{3v}$  form, which is reduced to 551.8 kJ mol<sup>-1</sup> at the MCPF-Douglas-Kroll level. Similarly, the relative energy of the  $D_{3h}$  form is lowered from 161.3 to 144.9 kJ mol<sup>-1</sup> while that of the staggered  $C_{3v}$  isomer is raised by only 11.1 kJ mol<sup>-1</sup> when comparing non-relativistic RHF and the MCPF-Douglas-Kroll data.

Finally, if we take the almost identical results from the CCSD(T)/BS6 and all-electron MCPFDouglas-Kroll calculations as the reference, it is obvious that the B3LYP/BS6 data show the best agreement. The maximum deviation amounts to some 25 kJ mol<sup>-1</sup> and occurs for the high energy O<sub>h</sub> isomer. Thus, we conclude that the most efficient way to incorporate relativistic effects seems to be the use of an RECP. If the valence basis set is large enough it even does not really matter which one is being used. The economical benefits of an RECP also allow the geometries to be readily optimized, even when expensive electron correlation methods are included. The correlation problem is best solved using a conventional method such as CCSD(T), while one should be very cautious about the popular MP2 approach. Much cheaper, but only slightly less accurate seems to be the use of the Hartree-Fock/density functional hybrid B3LYP, while the pure DFT methods show a slightly inferior performance.

## Acknowledgements

This work was supported by the Gesellschaft von Freunden der TU Berlin and the Fonds der Chemischen Industrie. Computer time was provided by the Konrad-Zuse Zentrum für Informationstechnik Berlin. BFY's stay in Berlin, during which much of this work was carried out, was made possible by the generous allocation of sabbatical time by the University of Tasmania and the support of Prof. H. Schwarz. Finally, we are grateful to Prof. K. Seppelt for pointing out this problem to us.

## References

1. R. J. Gillespie and I. Hargittai, *The VSEPR Model of Molecular Geometry*, Allyn and Bacon, Boston, 1991.
2. M. Shen, H. F. Schaefer III, and H. Partridge, *J. Chem. Phys.*, **98**, 508 (1993).
3. S. K. Kang, H. Tang, and T. A. Albright, *J. Am. Chem. Soc.*, **115**, 1971 (1993).
4. N. Tanpipat and J. Baker, *J. Phys. Chem.*, **100**, 19818 (1996).
5. D. Andrae, U. Häussermann, M. Dolg, H. Stoll, and H. Preuss, *Mol. Phys.*, **80**, 1431 (1993).
6. P. H. Hay and W. R. Wadt, *J. Chem. Phys.*, **82**, 299 (1985).
7. W. J. Stevens, M. Krauss, H. Basch, and P. G. Jasien, *Can. J. Chem.*, **70**, 612 (1992).
8. *ADF, Version 2.1*, Department of Theoretical Chemistry, Vrije Universiteit, Amsterdam, The Netherlands.
9. S. Huzinaga and M. Klobukowski, *J. Mol. Struct.*, **167**, 1 (1988).
10. W. J. Hehre, L. Radom, and P. v. R. Schleyer, *Ab Initio Molecular Orbital Theory*, John Wiley & Sons, New York, 1986.
11. *TURBOMOLE, Version 2.3.5*, Biosym Technologies, Inc., San Diego, CA, 1994.
12. M. J. Frisch, G. W. Trucks, H. G. Schlegel, P. M. W. Gill, B. G. Johnson, M. A. Robb, J. R. Cheeseman, T. A. Keith, G. A. Petersson, J. A. Montgomery, K. Raghavachari, M. A. Al-Laham, V. G. Zakrzewski, J. V. Ortiz, J. B. Foresman, C. Y. Peng, P. Y. Ayala, W. Chen, M. W. Wong, J. L. Andres, E. S. Replogle, R. Gomperts, R. L. Martin, D. J. Fox, J. S. Binkley, B. J. DeFrees, J. Baker, J. P. Stewart, M. Head-Gordon, C. Gonzales, and J. A. Pople, *Gaussian-94*, Revision B.3, Gaussian, Inc., Pittsburgh, PA, 1995.
13. *MOLPRO* is a package of *ab initio* programs written by H.-J. Werner, and P. J. Knowles, with contributions from J. Almlöf, R. D. Amos, M. J. O. Deegan, S. T. Elbert, C. Hampel, W. Meyer, K. Peterson, R. Pitzer, A. J. Stone, P. R. Taylor, and R. Lindh.
14. J. E. Rice, H. Horn, B. H. Lengsfeld, A. D. McLean, J. T. Carter, E. S. Replogle, L. A. Barnes, S. A. Maluendes, G. C. Lie, M. Gutowski, W. E. Rudge, P. A. Sauer, R. Lindh, K. Andersson, T. S. Chevalier, P.-O. Widmark, D. Bouzida, J. Pacansky, K. Singh, C. J. Gillan, P. Carnevali, W. C. Swope, and B. Liu, *Mulliken 2.0*, IBM Almaden Research Center, San Jose, CA, 1996.
15. A. D. Becke, *Phys. Rev. A*, **38**, 3098 (1988).
16. J. P. Perdew, *Phys. Rev. B*, **33**, 8822 (1986).
17. A. D. Becke, *J. Chem. Phys.*, **84**, 4524 (1986).
18. C. Lee, W. Yang, and R. G. Parr, *Phys. Rev. B*, **37**, 785 (1988).
19. A. D. Becke, *J. Chem. Phys.*, **98**, 5643 (1993). In *Mulliken*, a slightly modified version of the B3LYP functional is implemented: instead of the VWN functional, the local correlation functional of J. P. Perdew, and Y. Wang [*Phys. Rev. B*, **45**, 13244 (1992)] is used. For a discussion of the effect of different formulations of the B3LYP functional, see: R. H. Hertwig and W. Koch, *Chem. Phys. Lett.*, **268**, 345 (1997).
20. T. Ziegler, V. Tschinke, E. J. Baerends, J. G. Snijders, and W. Ravenek, *J. Phys. Chem.*, **93**, 3050 (1989).
21. K. Anderson, M. R. A. Blomberg, M. P. Fülscher, V. Kellö, R. Lindh, P.-A. Malmquist, J. Noga, J. Olsen, B. O. Roos, A. J. Sadlej, P. E. M. Siegbahn, M. Urban, and P.-O. Widmark, *MOLCAS-3*, University of Lund, Sweden, 1994.
22. D. P. Chong and S. R. Langhoff, *J. Chem. Phys.*, **84**, 5606 (1986).
23. R. L. Martin, *J. Phys. Chem.*, **87**, 750 (1983).
24. M. Douglas and N. M. Kroll, *Ann. Phys.*, **82**, 89 (1974).
25. B. A. Heß, *Phys. Rev. A*, **33**, 3742 (1986).
26. B. A. Heß, *Ber. Bunsenges. Phys. Chem.*, **101**, 1 (1997).
27. Brian.Yates@utas.edu.au.
28. R. B. Ross, J. M. Powers, T. Atashroo, W. C. Ermler, L. A. LaJohn, and P. A. Christiansen, *J. Chem. Phys.*, **93**, 6654 (1990).
29. E. Eliav, U. Kaldor, P. Schwerdtfeger, B. A. Heß, and Y. Ishikawa, *Phys. Rev. Lett.*, **73**, 3203 (1994).
30. M. Seth, P. Schwerdtfeger, M. Dolg, K. Fægri, Jr., and B. A. Heß, U. Kaldor, *Chem. Phys. Lett.*, **250**, 461 (1996).
31. M. Kaupp, *J. Am. Chem. Soc.*, **118**, 3018 (1996).